NASA Technical Memorandum 107311

Ignition of Cellulosic Paper at Low Radiant Fluxes

K. Alan White
Lewis Research Center
Cleveland, Ohio

August 1996

National Aeronautics and
Space Administration

IGNITION OF CELLULOSIC PAPER AT LOW RADIANT FLUXES

Summary

The ignition of paper samples by low level thermal radiation is investigated herein. At flux levels below 10 Watts/cm^2, other investigators (*Simms, Weatherford*) have observed that autoignition of paper does not occur. Thus, an experimental study of piloted ignition of paper is described. The objective of this work is to understand ignition of cellulosic paper by low level thermal radiation, with application to fire safety aboard orbiting spacecraft. Also, better understanding of the effects of gravity and buoyant flows on the ignition process is sought.

The chemistry of cellulose combustion is briefly reviewed. As cellulosic fuels are heated, H_2O, CO, and CO_2 are liberated first. After these, volatile organics such as acetaldehyde, acrolein, and methanol are liberated in trace amounts as the cellulose polymer pyrolyzes and decomposes. Temperature profiles during heating are presented, which indicate some of the endothermic and exothermic steps before ignition. Inspection of these profiles indicate that ignition temperatures are consistent with igniting these more volatile organics.

The main experimental parameters investigated are incident radiant flux, the degree of focussing of the radiative heat source, the optimal placement of a pilot ignition source, and the effects of various normal gravity orientations on ignition. It is observed that the incident radiative flux (in W/cm^2) has the greatest influence on ignition time. For a given flux level, a narrower (focussed) Gaussian source is found to be advantageous to a broader, lower amplitude Gaussian heat source. Positioning of a pilot ignition source is observed to influence ignition, but the precise effects depend on the transient heating profile at the fuel surface.

To better understand ignition of paper in microgravity, the apparatus was oriented to investigate various buoyant flow directions. Ignition was more readily achieved and sustained with the fuel sample horizontal, most likely because of growth of a boundary layer of volatilized decomposition products. Orientation relative to gravity was also observed to measurably influence ignition times, with horizontal fuel orientations igniting more rapidly.

Smoldering combustion of doped filter paper samples was briefly explored. It was observed that a focussed radiation source is preferred to initiate smoldering. The temperatures observed indicate that surface reactions are important, and can compete with gas phase reactions.

Introduction

One objective of the NASA microgravity science program is to investigate the combustion of solid samples in microgravity. Such research furthers understanding of fire propagation both in orbiting spacecraft and in normal gravity, and contributes to improved spacecraft fire protection systems. Since paper will be present in any manned spacecraft, combustion of cellulosic materials in normal and microgravity has been investigated previously (*Olson, Sacksteder*).

Although much work has been done at higher irradiances (above 15 W/cm^2), knowledge of cellulosic ignition at lower irradiances is lacking. These lower heat levels are more representative of sources likely to exist in an orbiting spacecraft. At low flux levels, autoignition of cellulose does not occur. Also, a microgravity study aboard the NASA LeRC Learjet indicated that radiative ignition at low fluxes was difficult to achieve. Thus, further understanding of the parameters affecting piloted ignition is addressed herein.

This article addresses a limited characterization of ignition of one type of ashless filter paper. In support of a NASA flight experiment, a systematic study of ignition of paper with a radiating source is reported. The objective of this study was to understand ignition of ashless filter paper using a halogen lamp to heat the paper and a pilot to ignite the gas phase products, and thus sustain a gas-phase flame. Since this effort was in support of a shuttle flight project, there were competing demands for the experimental hardware, and extensive reproducibility testing could not be conducted.

Discussion of Previous Work

Brief reviews of radiative ignition and combustion of cellulose are in order. The general criteria necessary for autoignition or piloted ignition to be sustained from a radiative heat source can be summarized (*Kashiwagi, 1981*):

1) a fuel and oxygen mixture within or near the flammability limits must be available in the gas phase;

2) the gas phase temperature must be high enough to initiate and sustain gas phase chemical reactions;

3) heat losses from the gas phase must be low enough so that chain reactions can be sustained, with sufficient heat transfer from the flame to the fuel.

In the study reported herein, a Kanthal wire resistively heated to nearly 1100 K served as a pilot to ignite the combustible mixture. For piloted ignition, criterion (2) can be restated. If the pilot is at a sufficiently high temperature to ignite the gas phase mixture, and is located within a flammable mixture, the second criterion is satisfied.

One of the principal advantages of piloted ignition is that less energy would normally be required to achieve ignition. For low-flux (below 10 W/cm^2) heating of red oak, Kashiwagi (*1979*) observed piloted ignition in 25 - 35% of the time required for autoignition. For autoignition, irradiance must be sufficiently high to satisfy (2). With piloted ignition, a sufficiently high temperature is maintained near the pilot. This assumes that it is optimally located in the gas phase, which is investigated herein.

Combustion of Cellulose

Some knowledge of the combustion of paper is needed to ascertain when the first criterion can be satisfied. To a first order, paper can be modelled as a composite of lignin, cellulose, and hemicellulose. An in-depth overview of pyrolysis and combustion of cellulose is given elsewhere (*Shafizadeh*).

When paper is heated in the absence of a flame, one can readily observe that the paper turns brown, and then blackens, resulting in a much weaker structure. This solid-phase decomposition is termed pyrolysis, and can occur before a visible flame is present. When exposed to flame or a

sufficiently high temperature, the paper will be consumed, leaving only a black charry residue and ash. This involves gas-phase reactions, collectively called combustion. Pyrolysis reactions will normally occur before combustion, but may not occur at extremely high heat fluxes (*Martin*).

Cellulose pyrolyzes by at least two mechanisms. Below 600 K, these steps occur during pyrolysis: (a) cellulose begins to depolymerize; (b) adsorbed and bound water are liberated; (c) free radicals are formed; (d) CO and CO_2 are liberated; and (e) a highly reactive char is formed. That is, cellulose does not burn directly. Rather, it decomposes with temperature, liberating volatile compounds and leaving a reactive char. This char phase can then be consumed in the presence of a flame. Above 600 K, heavier compounds such as levoglucosan, furanose, polysaccharides and oligosaccharides are produced, which can then vaporize with sufficient heat. These compounds are somewhat tar-like, leaving traces of a sticky residue after combustion.

In conjunction with the heavy sugars, more volatile compounds are also generated. The gas phase composition is predominantly CO, CO_2, and H_2O. After these, one study (*Martin, 1965*) measured acetaldehyde in the greatest concentration, followed by acrolein, methanol, furan, acetone, ethylene, and methane. That study used a constant irradiance of 18.4 W/cm^2; herein, area-averaged (*i.e.*, not constant) irradiances between 4 and 9 W/cm^2 are used.

It has been observed that the rate of volatile generation depends on irradiance (flux) level, as expected. Due to competing pyrolysis reactions, the volatile composition also varies greatly with flux level. Hence, accurate prediction of the volatile composition in the present work is impossible without analyzing the volatiles at the irradiance level of interest. This fact is further discussed by Martin, who states that the "distribution of products is a function of the manner in which the cellulose is heated." The manner of heating includes the type of pilot used as well as the heating profile.

For the current work, it is assumed that CO, acetaldehyde, acrolein, methanol, and levoglucosan are the principal combustible gases. Spontaneous ignition (autoignition) of CO in air occurs around 900 K. Acetaldehyde autoignites around 460 K; acrolein, above 500 K; methanol, above 750 K; and furan, above 1000 K. These values are tabulated elsewhere (*Glassman, 1987*). Based on the structure of levoglucosan, it would be expected to autoignite at an even higher temperature. These values are for autoignition; piloted ignition would occur at lower temperatures. For low flux radiative heating of cellulose, where the gas phase temperatures are low (400 - 700 K), it is assumed that acetaldehyde and acrolein will ignite most readily, given their availability and lower ignition temperatures. Since CO is the most plentiful combustible, its combustion may help to sustain gas-phase ignition, once achieved.

The exothermicity of various steps must be discussed. The initial pyrolysis of cellulose is endothermic, and evaporation of levoglucosan and the volatiles released by pyrolysis is highly endothermic (*Shafizadeh*). Since these volatiles are necessary for gas phase ignition, sufficient heating of the paper fuel must occur before ignition. A highly endothermic step during a period of constant heating implies that d^2T/dt^2 becomes negative. Since ignition can occur after sufficient release of combustible gases, a change in dT/dt may be evident just prior to ignition, due to release of volatiles. Kashiwagi (*1992*) reports that the overall pyrolysis reaction is endothermic (570 J/g), while gas phase combustion is exothermic (-5700 J/g).

Overall Surface Reactions

The reactions leading to formation of ignitable volatiles have been addressed. Other surface reactions during heating can also affect ignition. The end product of pyrolysis is a highly reactive

char. Available O_2 molecules are chemisorbed on the char, as measured by thermogravimetry (*Shafizadeh*). The carbonaceous char is oxidized to give CO and CO_2, both exothermic reactions (*Kashiwagi, 1987*). In a study of ashless filter paper, Kashiwagi (*1992*) observed that more CO_2 was generated from oxidation of the char than from gas phase oxidation. Furthermore, Shafizadeh reported the enthalpies for combustion of a cellulosic filter paper to be -1050 cal/g for the char, and -3093 cal/g for the gaseous volatiles. This shows that the consumption of O_2 by the surface oxidation of the char can be significant. At lower O_2 concentrations, the surface pyrolysis reactions are increased relative to the gas-phase combustion of volatiles. That is, gas phase combustion can be inhibited if sufficient O_2 is not available, such as at low concentration or due to low air flow rates.

If the ignition of combustible volatiles is sufficiently inhibited, surface pyrolysis can consume the char. This is known as smoldering combustion. Smoldering can be predominant at low O_2 levels, and can be catalytically promoted by the presence of Na^+ or K^+ ions.

In summary, radiative ignition of paper is determined by the local O_2 level, by generation of sufficient combustible volatiles, by a sufficiently high temperature to ignite the volatiles, and by the continuing availability of volatile species after ignition. If volatile pyrolysis products are not supplied to the gas phase after ignition, extinction of the flame will occur, although surface smoldering may continue.

Experimental Apparatus

The effort described herein is in support of a NASA flight experiment conducted on STS-75 in March 1996. The experiment is known as RITSI, for "Radiative Ignition and Transition to Spread Investigation." The apparatus is designed to fly in an enclosed volume similar in size and function to a laboratory glovebox. Such glovebox experiments are characterized by low cost, small physical size, quicker access to space, and shorter development times, relative to other flight opportunities. A glovebox experiment is allotted 100 W of dc power, split among +24, ±12, and +5 V supplies. This work examines ignition of paper using less than 80 W of dc power. In this study, up to 60 W from the 24 V supply, and up to 20 W from the 5 V, are available as ignition sources.

The RITSI apparatus flown on STS-75 is shown in Fig. 1. A functionally similar "engineering model" of the flight hardware was used herein. The test section is a rectangular flow duct 95 x 85 mm in cross section, and 180 mm long. Ambient air is drawn through the duct using a centrifugal fan at the outlet, sized for flow velocities up to 5 cm/s. Fine (60 and 100) mesh screens are used at the duct inlet and outlet. Previous smoke particle testing has shown that the proper combination of outlet screens in series can eliminate swirling effects induced by the fan. Flow velocities in the duct test section are calibrated indirectly using a hot wire anemometer.

A fuel sample holder, also 180 mm long, separates the flow duct into two volumes. The sample holder (not shown for clarity) is installed in the top of the flow duct, resulting in a vertical fuel sample for the Fig. 1 orientation. All tests used an ashless filter paper, Whatman™ 44, as the fuel. The paper samples, nominally 75 x 125 mm, were glued onto the sample holder, which was then held securely in the flow duct by 14 electrical pin connectors. The flow duct allowed the sample holder to be placed in one of two positions, one centered in the flow duct, and one closer to a halogen lamp.

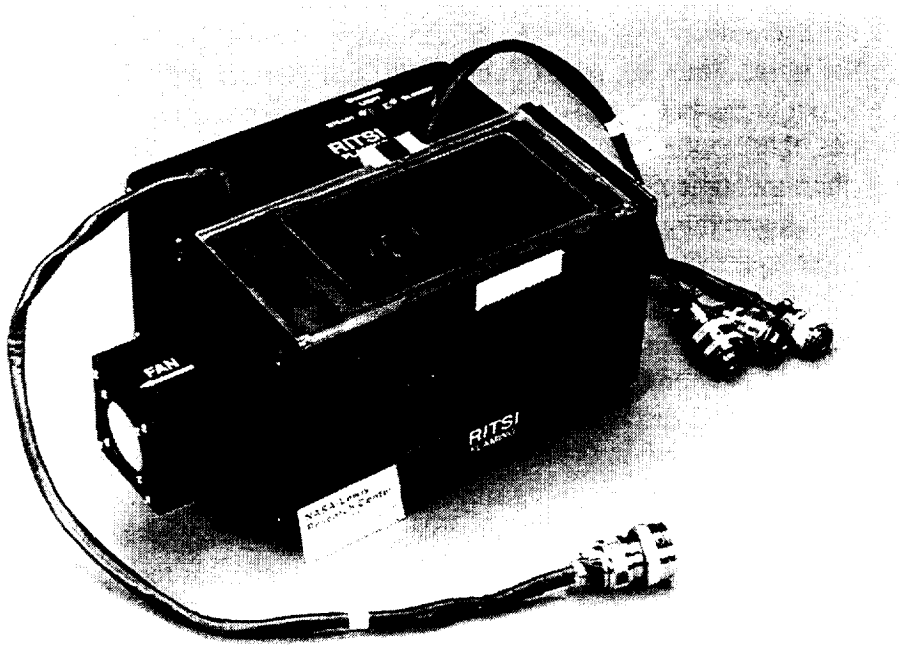

C-95-4728

Figure 1 — Experimental Apparatus

The halogen lamp volatilized the paper sufficiently for gas phase products to be ignited. The paper samples are irradiated by a tungsten-halogen heat lamp. The lamp is visible at the back of the Fig. 1 flow duct, opposite the front window. The lamp is housed outside the flow duct, and shines through a 3 mm thick quartz window which is mounted flush in the duct wall, so as not to disturb duct air flow. As shown in Fig. 2, a 33 gauge Kanthal igniter wire runs across the center line of the paper, between the paper and the heat lamp. The igniter geometry included an 18 mm long, straight Kanthal portion, which was spot welded to copper lead wires. The copper leads

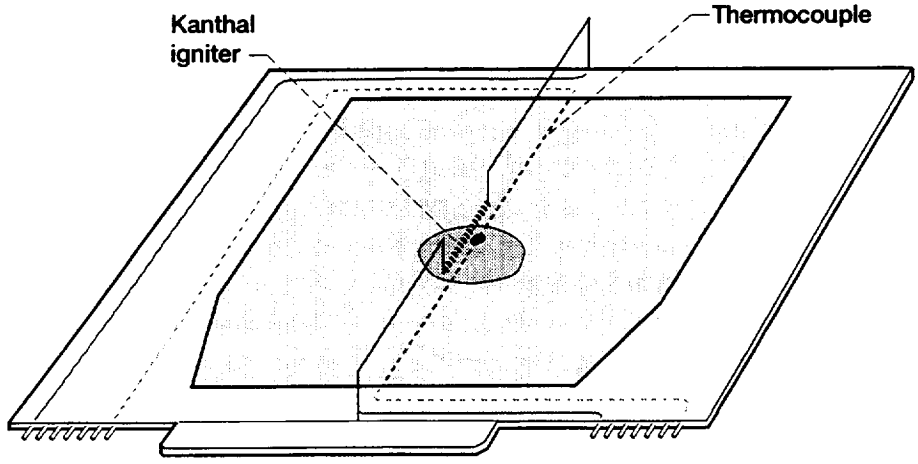

Figure 2 — Location of Igniter and Thermocouple

could be bent to position the Kanthal wire at varying distances from the surface. For the present study, done in normal gravity and 21% O_2, it was not possible to ignite untreated filter paper without an igniter wire. Thus, for sake of clarity, the term *igniter* will always refer to the Kanthal igniter wire, and not to the halogen lamp. Although the lamp can autoignite the filter paper at higher irradiances, the Kanthal pilot igniter was necessary at the low flux levels of this study.

A Type K thermocouple ran parallel to the igniter wire, but on the opposite side of the paper. This allowed the halogen lamp to irradiate the paper surface, but not the thermocouple bead, until a hole had burned through the paper. The thermocouple thus recorded the temperature history at the midpoint of the paper.

The apparatus thus allowed for variable separation (nominally 4 and 5 cm) between the tungsten-halogen filament and the paper. At 4 cm, the nominal paper area irradiated was 2.80 cm^2; at 5 cm, 3.92 cm^2. (Further discussion of spot size is deferred to the *Results* section.) Also, the Kanthal igniter could be placed on the surface of the paper, or anywhere up to 10 mm away. The halogen heat lamp irradiated the paper, causing vaporization and pyrolysis reactions to occur. When sufficient vaporized products had accumulated in the gas phase, the Kanthal wire would ignite the gas-phase mixture, leading to sustained flame spread consuming the paper.

The ignition and flame spread processes were filmed by video camera at 30 frames/sec. One camera was focused on the paper surface, viewing through the front window of Fig. 1. This view clearly showed pyrolysis, ignition, and the visible flame spread during a test. A second camera monitored air velocity, lamp power, and thermocouple LED displays, with a display update rate of 3 Hz. These cameras recorded all data reported and discussed herein, which consisted of both visual records and temperature histories at the focal point of the halogen source.

Experimental Procedure

The procedure for all data discussed below involved first preparing a new fuel sample for each test. After cutting to shape, it was then necessary to coat a portion of the paper with a soot spot, nominally 15 - 18 mm diam. The soot was generated by burning an ordinary household kerosene lamp, the deposited soot being scraped off the glass globe. The soot so collected was applied to the paper with a cotton swab, using sufficient pressure to visibly darken the paper as much as possible. The soot spot was only applied at the focal area of the halogen lamp, and allowed for higher absorption in the near infrared. The spot was kept small to minimize changes in the thermal or physical properties (other than absorptivity) of the paper. If a soot spot were not applied, the paper could not be ignited even at 15 W/cm^2, well above the power capabilities of the shuttle glovebox.

The paper was next glued to the sample holder. Once installed, the thermocouple was adjusted until the bead touched the surface of the paper. Next, the copper leads of the igniter wire were adjusted such that the Kanthal igniter was straight and unstressed, and parallel to the paper surface, but 3 - 5 mm from the paper. As shown in Fig. 2, the Kanthal igniter and the soot spot were on the same side of the paper, with the thermocouple on the opposite side. The sample card was installed in the flow duct, and was then inspected to check the igniter wire distance after insertion. The duct was sealed, and the fan started to draw air through the test section at 5 cm/s.

Once a sample was installed, the halogen lamp power was preset by a calibrated potentiometer. Video recorders and timers were initialized, and the halogen lamp was energized to the predetermined power. The halogen lamp was controlled by a timer circuit to stay on for 23 sec. After

the halogen lamp was energized, the Kanthal igniter was manually energized, and remained energized until a gas phase flame was observed.

Proper interpretation of the data requires knowledge of the lamp radiation incident on the paper. This was determined experimentally for various input power levels. The halogen lamp was energized, and a flux gage was positioned in a plane 4 cm from the lamp, where the paper sample

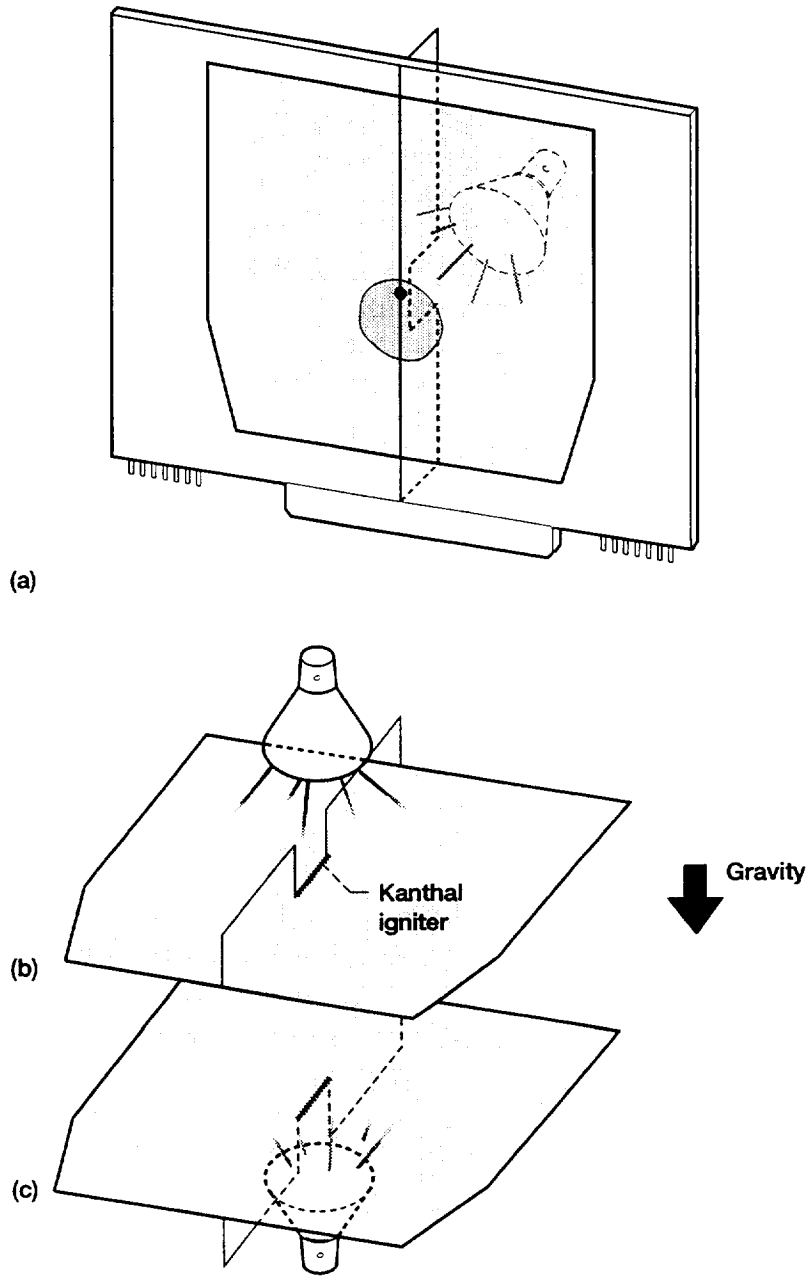

Figure 3 — Sample Orientations in Normal Gravity
(a) Vertical; (b) Horizontal; (c) Horizontal

would otherwise be. The lamp was then repositioned to obtain radiant flux (in W/cm^2) as a function of position. The lamp intensity was found to be nearly Gaussian in both orthogonal directions. This procedure was done at 40, 50, and 60 W input power. Using the origin point as well, incident radiation was determined by the equation $y = 0.00852x^2 - .02506x + 0.067$, where x denotes electrical input to the lamp, and y, incident radiation (both in Watts). This procedure accounted for losses such as heating of the lamp housing and surrounding hardware, and any radiation losses in the direction *away* from the plane of the paper.

The above equation indicates the radiation incident on a paper sample 4 cm away. Although an α of 0.95 has been reported for soot (*Siegel*), the absorptivity of the soot-darkened area would be less, perhaps 0.9 - 0.92. The effective absorption of the paper over the entire soot spot could not be readily measured. Additionally, incident radiation is overestimated due to some gas-phase absorption by volatilized species. In 4 W/cm^2 heating of red oak, Kashiwagi (*1979*) reported that volatilized species could attenuate the radiation by up to 20% at ignition. To first order, the initial volatiles from filter paper would be similar, namely CO, CO_2, and H_2O. Although incoming radiation is unlikely to be attenuated 10 or 20% in 5 sec by these species, there is some (undetermined) attenuation of the halogen lamp.

Although the fan drew ambient air through the flow duct at a constant 5 cm/s, buoyant flow is predominant. The magnitude of the buoyant gases upward probably significantly exceeds the 5 cm/s forced flow. Though a definitive prediction is beyond the scope of this article, buoyant flows within the flow duct on the order of 50 cm/s might be expected. Thus, the fundamental differences between buoyant flows in normal gravity and microgravity must be considered.

In an effort to predict behavior in microgravity, the apparatus was tested in three unique 1g orientations, shown in Fig. 3. The intent of this testing was to vary the buoyant flow of vaporized products relative to the lamp and igniter. In the baseline case, shown in 3a, the paper surface was vertical, with the lamp beam oriented horizontally. In this case, the vaporized products would tend to rise toward the top of the paper. In 3b, the hardware was oriented with the paper horizontal, with the lamp shining down, in the direction of the gravity vector. In this case, the buoyant gases would rise toward the lamp and igniter, and one would intuitively expect this to be a favorable orientation, due to a higher concentration of volatiles near the igniter. In the *c* orientation, the paper was again horizontal, but with the lamp radiating upward, and buoyant flow would be predominantly away from the lamp and Kanthal igniter.

The series of tests performed are indicated in Table I. The relation between lamp position (in cm) and radiant flux incident on the paper is discussed below. The only igniter separations investigated were 3 and 5 mm. At distances closer than 3 mm, it becomes harder to discern whether the ignition process is truly radiative, or more similar to piloted ignition. Given the 60 W power constraint, it was very difficult to reliably ignite the paper much beyond the 5 mm distance, although this was not investigated in detail. The *a, b, or c* notation refers to Fig 3a, 3b, or 3c, respectively. The Series **8** tests involved using a common glue stick to paste two sheets together, thus creating a fuel sample twice as thick. Ignition of these samples was impossible, given the power constraints imposed.

The Series **9** and **10** tests were an investigation of the time to onset of smoldering. For these, NIST researchers (*Kashiwagi* and coworkers) doped the Whatman™ 44 paper with potassium acetate, which helps to promote smoldering. Neither the soot spot nor the igniter were necessary to initiate smoldering, and were not used. These tests are discussed separately.

Test Series	Lamp (cm)	Igniter (mm)	Gravity Vector†
1	4	3	a
2	4	5	a
3	4	5	b
4	4	5	c
5	4	5‡	b
6	5	3	a
7	5	5	a
8	5	5*	b
9	4	n/a	a
10	5	n/a	a

† - See Figure 3.
‡ - Kanthal igniter preheated for ≈ 2 sec
* - Double thickness of paper tested; see text.

Table I — Experimental Test Matrix

Discussion of Error Sources

To properly interpret the data, several sources of experimental error should be discussed. These are of two types—subtle variations during sample preparation, and subtle changes in operating procedures during a test. Although these were appreciated during the testing, design and schedule constraints precluded totally eliminating them.

One potential error is the uniformity of the soot spot. No template was used to position the soot spot in precisely the same location in all tests. Second, the method of applying the soot with a cotton swab was not completely reproducible, and the paper was not uniformly coated over the entire spot. Since the absorptivity of soot is near 0.95, and that of paper is perhaps 0.15 (*Siegel*), absorption of the incident radiation could vary between tests, even with constant *input* power. The magnitude of this effect cannot be accurately assessed.

Another source of error resulted when the sample card was inserted into the flow duct. Because of the design, slight bending of the sample card would occur. Two effects could result. One, the centerline thermocouple could be displaced as much as 0.5 mm from the surface of the paper. More significantly, the igniter separation could also vary by 0.5 mm, which would presumably be more significant at the 3.0 mm igniter distance. Therefore, a stated igniter separation of 3.0 mm actually indicates 3.0 ± 0.5 mm.

Since the experimental procedure was conducted manually, subtle variations in operating procedure could occur. For all data presented below, time zero is taken when the halogen lamp was first energized manually. After energizing the lamp, the igniter wire was then immediately energized manually. Since the igniter wire also radiantly heated the sample, a typical operator variance of perhaps 0.5 sec would change the temperature profile of the sample before ignition, particularly when ignition occurred in 4 - 5 sec. For the Series **5** tests where the igniter was energized nominally 2 sec before the lamp, variations in the 2 sec interval are especially significant. This can be seen in Fig. 7, discussed later.

Another source of procedural error was in the energizing of the halogen lamp. The LED display indicated that a steady state current was not reached for 1.1 - 1.2 sec. The transient response was not analyzed, but included an overshoot above the final steady state current, with asymptotic behavior presumed after the overshoot. Because of the current overshoot and design constraints, it was necessary to manually increase the Wattage for desired steady state powers above 53 W (8.2 W/cm^2 incident). This was effected by adjusting a dial potentiometer to the desired steady state current. The ramping up to steady state values above 54 Watts (8.5 W/cm^2 incident) was variable, and took from 1 - 2.5 sec.

The implication of these variations in operating procedure is that the precise incident radiation was not known in the first 1.1 sec. Also, at stated incident fluxes above 8.2 W/cm^2, the radiated energy could vary between tests because of variable ramp-up rates. Thus, the actual radiant flux above 8.2 W/cm^2 was variable before ignition. For these reasons, more data scatter would be expected at the highest fluxes (shortest times).

It is necessary to understand what the centerline thermocouple was actually indicating. As shown in Fig. 2, the bead is located on the surface of the paper, within the soot-darkened area, but initially shielded from the halogen lamp and igniter. When the lamp was energized, a hole would burn through the paper at the focal point of the lamp, and would grow to as large as 10 mm. As the hole grew, view factors from the lamp and igniter to the thermocouple increased. However, under similar conditions, Kashiwagi (*1979*) found that 4 W/cm^2 radiation caused no perceptible change in thermocouple reading, due to bead size and reflectivity. Thus, the thermocouple indicated a surface temperature only for the first 1 - 2 sec, but was apparently accurate despite radiation from the lamp.

As mentioned, the thermocouple bead could move as much as 0.5 mm after installing the sample card. Also, the igniter position could vary ± 0.5 mm relative to the paper surface. Once ignited, temperature gradients in a flame can typically be 100 K/mm. Thus, *after* ignition, the indicated temperature could vary up to 100 K between separate tests, due to a 1 mm uncertainty in positioning. However, for a given test, the thermocouple and igniter position are presumably constant throughout the ignition process. Thus, although absolute temperatures reported herein have a spurious meaning after ignition, the derivative dT/dt would remain unaffected by positioning uncertainties. Since the point of ignition was determined as a sudden change in dT/dt, as shown in Fig. 4, ignition times can be accurately determined, in spite of the spurious indication of the thermocouple.

In summary, variations in the soot spot and variability in energizing the halogen lamp and igniter would affect the total energy incident on the fuel before ignition, even with a constant steady state power level. These error sources and other factors make determination of temperature after ignition quite problematic, although the derivatives, dT/dt, and especially d^2T/dt^2, would be much less impacted. Graphical interpolation in Figs. 4 - 7 allows determination of the point of ignition within ± 0.05 sec, less than the LED update rate. A rigorous error analysis would be nearly impossible, and beyond the scope of this paper.

Experimental Results

For each test series of Table I, the data recorded included a video record of the ignition and flame spread process, temperature history at the midpoint of the paper, and air flow rate through the duct. Unless noted, the bulk velocity was a constant 5 cm/s for all tests. No changes in the ignition

process were observed at lower velocities. Conversely, buoyant flows of the order of 50 cm/s influence both ignition and flame spread.

Incident Radiative Flux

As described previously, the power radiated from the tungsten-halogen lamp and incident on the paper is given by $y = 0.00852x^2 - .02506x + 0.067$, where x denotes electrical power input to the lamp. The flux gage procedure indicated that lamp intensity was near-Gaussian in both orthogonal directions. This procedure further revealed that the lamp irradiated an elliptical area, at both 4 and 5 cm, indicating an imperfect parabolic reflector. Elliptical eccentricity was 0.60 ± .03.

Since a Gaussian distribution mathematically extends to infinity, there is a somewhat arbitrary decision in assigning a spot size. For laser sources with a Gaussian distribution, it is common to define a spot size such that the intensity on the perimeter of the spot is $1/e^2$ (or 13.5%) of the maximum intensity at the centerline (*Eckbreth)*. For a Gaussian distribution, this choice of spot size equates to a beam containing 86% of the radiated power. This $1/e^2$ convention is used herein; to first order, this diameter is the approximate diameter of the initial hole burned in the paper by the halogen lamp. (The results presented below suggest that the lowest flux levels outside this spot size are insufficient to pyrolyze the paper). With this convention, the area of the ellipse is 2.80 cm^2 at 4 cm and 3.92 cm^2 at 5 cm.

Thus, for 60 Watts electrical power supplied to the lamp, calibration results indicate that 29.2 Watts is incident on the paper surface either 4 or 5 cm away. Using the $1/e^2$ convention, the *area-averaged* flux within the elliptical spot is 10.4 W/cm^2 at 4 cm, and 7.45 W/cm^2 at 5 cm. For comparison, the flux gage calibration indicates that the *peak* flux level at the center of the spot is about 19 W/cm^2 at the focal point of the lamp, 4 cm away. The radiative flux values reported herein are the *average* flux values. This is appropriate because fluxes lower than the peak flux also contribute to cellulosic decomposition.

The flux levels reported below are the flux levels incident on the paper, and do not account for the absorptivity of the soot spot (≈ 0.9 - 0.92) applied to the paper. Similarly, any gas phase absorption of the radiation by volatilized species (*Kashiwagi, 1979*) is neglected.

Temperature Profiles

The ignition time was determined by two methods. In examining the video record, a characteristic puff of smoke could be detected immediately before a sooty flame became visible. Although this puff was indicative of ignition, the more accurate method is to analyze a characteristic temperature change with time. Figure 4 shows such temperature histories for the Series **2** tests. (The incident flux levels, in W/cm^2, are noted by each curve.) As mentioned, the apparatus LED update rate was only 3 Hz. Instead, graphical interpolation was used to determine ignition to within ±0.05 sec. As indicated in Fig. 4, ignition is considered to occur when there is an instantaneous large increase in temperature.

Several observations are evident from Fig 4. First, ignition time increases with decreasing power level, allowing for experimental error. Second, temperature increases rapidly at ignition, and decays more slowly with time. Third, the peak temperature after ignition varies considerably.

To better predict ignition behavior in microgravity, similar testing was done for the hardware orientations shown in Fig. 3b and 3c (Test Series **3** and **4**). As shown in Fig. 3b, the buoyant flow of vaporized products is upward, toward the igniter wire and lamp. Results for Test Series **3** are

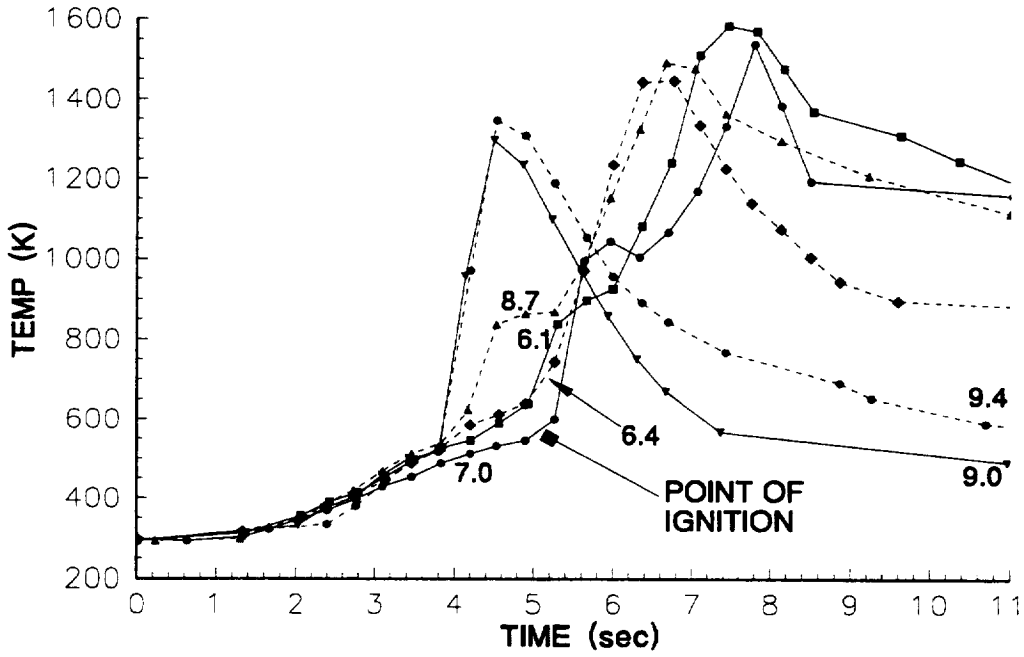

Figure 4 — Temperature Profiles for Test Series 2

presented in Fig. 5. As can be seen, the temperature profiles are much different in shape for Figures 4 and 5, even though the power levels are similar.

In the 3c configuration, buoyant flow is again upward, *away* from the igniter wire and lamp. These tests are shown in Fig. 6. Comparison of Figs. 4 - 6 shows that the general shape of the

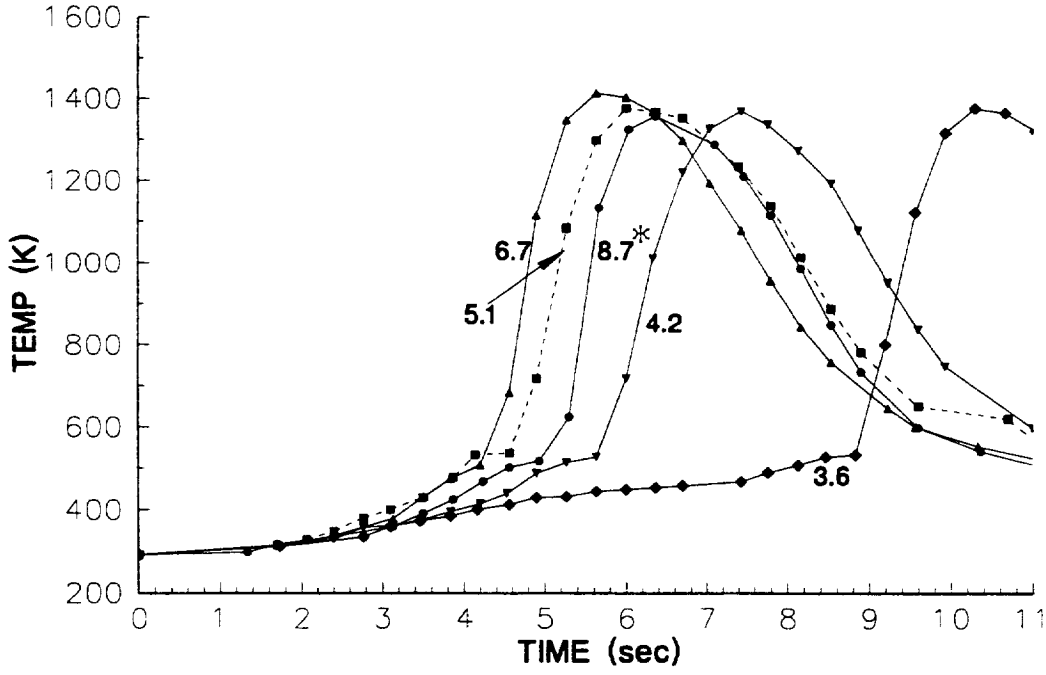

* Lamp Output Variable During Tests

Figure 5 — Temperature Profiles for Test Series 3

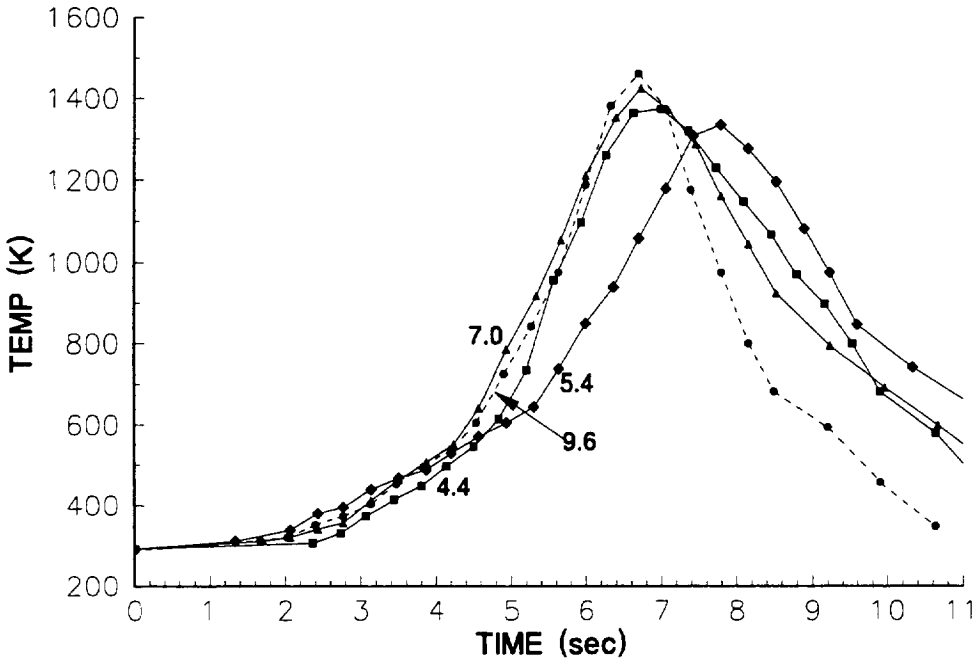

Figure 6 — Temperature Profiles for Test Series 4

temperature profiles begins to differ about 2 secs after energizing the lamp. Note that all variables—incident radiation, igniter separation, and distance from the lamp—are the same, and the ignition times are generally similar. It can be deduced that incident radiant flux alone is not sufficient to characterize ignition. It is clear that buoyant flows also affect the process. This will be addressed later.

Given that the Kanthal igniter takes a finite time to attain a steady-state temperature, one procedural modification was made. Energizing the igniter from a +5 V supply, the igniter temperature was observed to be near steady state after several seconds. Therefore, for the Series 5 tests, the Kanthal wire was manually energized about 2 seconds before energizing the lamp. This was done to ensure that the Kanthal wire was at a sufficiently high temperature before the most volatile products could dissipate by natural or forced convection. Though a longer preheat time would allow the igniter to attain a higher temperature, the thermal environment at the fuel surface would also be altered.

The preheated igniter temperature profiles are shown in Fig. 7. It should be noted that some of the initial temperatures in Fig. 7 are around 320 K, higher than the starting temperatures of 295 K in Figs. 4 - 6. This is due to radiant heating of the paper by the igniter wire. In Figs. 4 - 7, time zero has been defined as the time when the halogen lamp was energized.

Comparison of the general curve shapes of Figs. 5 and 7 is informative. All parameters are similar, and both show testing in the Fig. 3b orientation, with buoyant flow toward the Kanthal igniter. Preheating the igniter results in more rapid ignition at the same lamp power level. Secondly, inspection of the curves after the point of ignition indicates that the peak temperatures recorded are around 1300 K, rather than 1400 - 1500 K. Similarly, the temperature decays in a much different manner for the preheated tests than for all other tests. Although the physical significance of this is outside the scope of this paper, these observations suggest that preheating the

igniter fundamentally changes some aspect of the ignition process, rather than merely speeding up ignition. This will be discussed later.

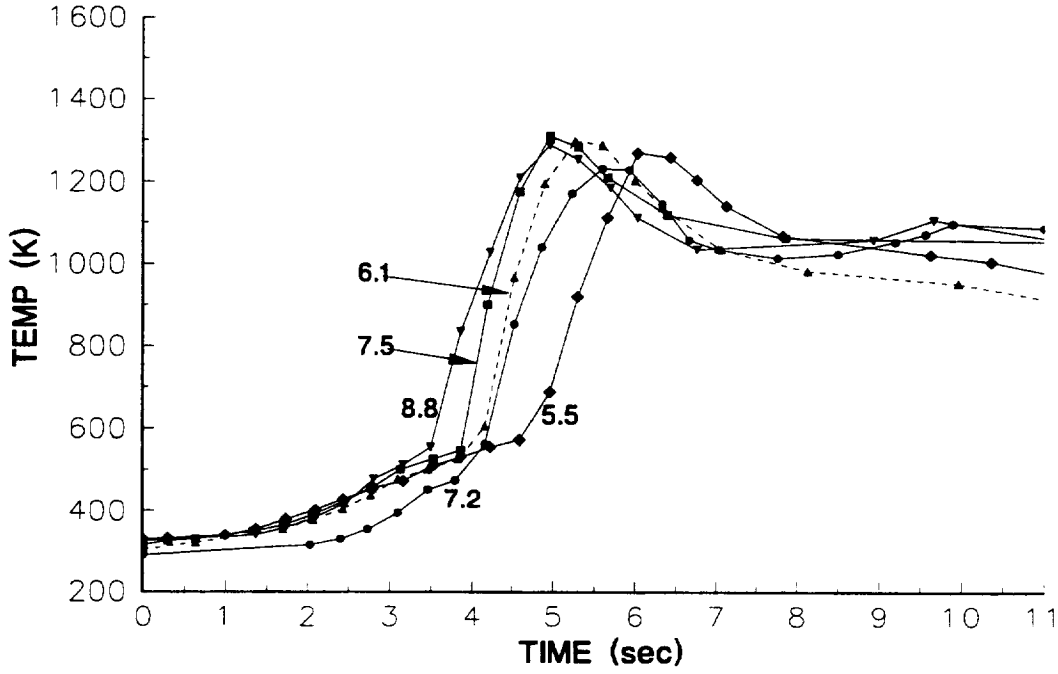

Figure 7 — Igniter Preheating for Test Series 5

Factors Affecting Ignition Time

For each temperature profile such as in Figs. 4 - 7, the point of ignition was determined graphically, as indicated in Fig. 4. The parameters impacting ignition, namely radiant flux, buoyant flows, and igniter separation, were next examined. The igniter distance was held constant, within positioning error, to 3 - 3.5 mm. The results are shown in Fig. 8 for both lamp positions.

It should be explained that the abscissa in Figs. 8 - 10 represents the total radiant flux (in W/cm^2) incident on the paper surface either 4 or 5 cm from the lamp at the point of ignition. As previously discussed, the lamp power began at 0 and reached steady state within 1.2 sec. That is, the radiated power would be considerably lower for the first 1.2 sec, but this could not readily be measured.

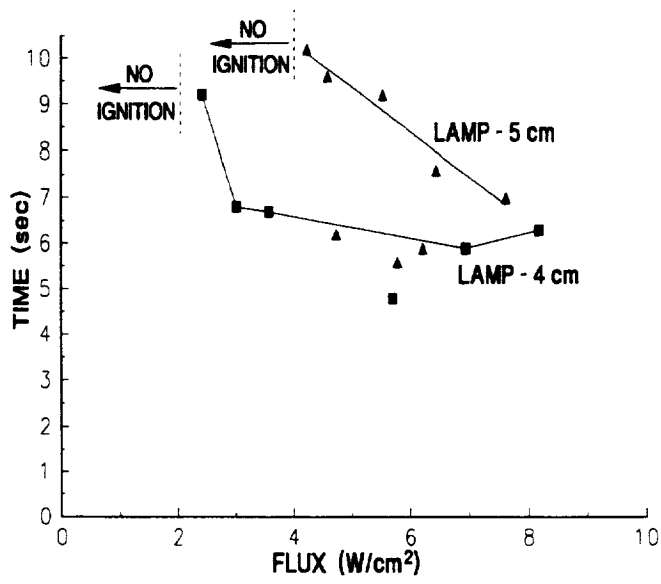

Figure 8 — Effect of Lamp Flux
(Igniter 3 mm from Surface)

It is readily apparent that for a given incident flux, ignition occurs more rapidly at the 4 cm distance. The tungsten-halogen lamp source contains a parabolic reflector with a focal length near 4 cm. The Gaussian distribution is narrower and higher at 4 cm; as the lamp beam diverges, the Gaussian distribution widens, with a lower centerline peak flux. Clearly, radiative flux alone cannot be used to predict ignition behavior.

Given the above, Fig. 8 indicates that a focussed lamp will ignite the paper more readily. It is also apparent that ignition time decreases with increasing incident thermal radiation, whether from a focussed source or not. Three data points (triangles) shown in Fig. 8 reveal significant scatter in the 5 cm tests. The scatter in these 3 tests is unexplainable, but may be due to excessive bending of the Kanthal igniter wire. At a nominal distance of 3 mm, a 1 mm error in the igniter distance could be quite dramatic, due to gradients around 100 K/mm in the gas phase.

Since Fig. 8 clearly indicated that a focussed lamp was more favorable at these flux levels, additional testing was done at the 4 cm distance. The optimum position of the Kanthal igniter was next examined. Results with nominal igniter standoffs of 3 and 5 mm are shown in Fig. 9. Again, ignition times are shorter at the higher power levels. A perhaps unexpected result is that ignition is seen to occur more quickly with an igniter farther from the surface. There are several possible explanations for this, which are deferred until *Discussion of Results.* It is also evident that ignition can be achieved at lower flux levels (2.4 *vs.* 6.1 Watts/cm^2) at the 3 mm position. The reasons for this are unknown.

Since Fig. 9 indicated that the preferred igniter separation was 5 mm with a focussed lamp source (4 cm location), some testing was done with the less-focussed lamp (5 cm) source. In the Series **7** tests, the igniter was positioned at 5 mm. Ignition could not be achieved at flux levels in the 5.5 - 8.5 W/cm^2 range. This contrasts with the Fig. 9 results, which indicate successful ignition between 2.4 and 8 W/cm^2 at the *3 mm* igniter position. Clearly, the optimum igniter location depends on the precise heating profile of the paper.

It was postulated that the unexpected behavior seen in the Series **6** and **7** tests might be attributable to the paper thickness. That is, since the paper samples are thin, heating the paper with the less-focussed lamp source could conceivably not generate sufficient volatilized products in the gas phase for ignition to occur. Therefore, in the Series **8** tests, the fuel sample was modified by pasting two filter paper sheets together with a common office supply glue stick. The resulting sample was merely twice as thick as in all other testing, with twice as much fuel present within the 3.92 cm^2 elliptical spot. This would thus allow for increased volatile generation rates upon heating the

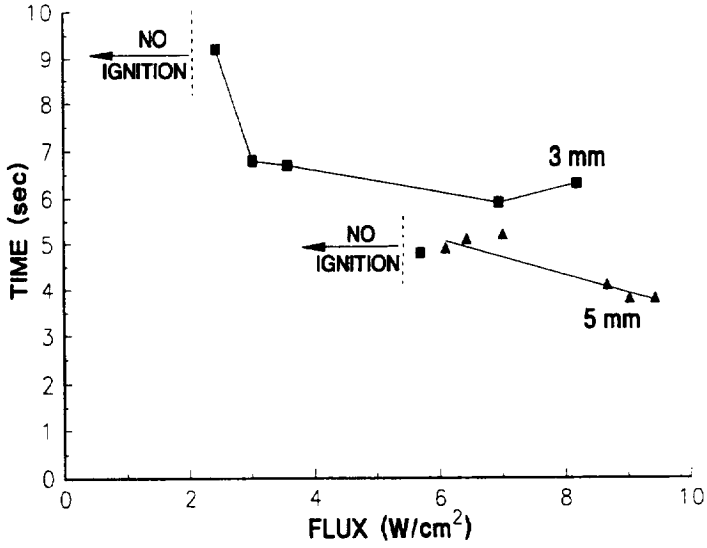

Figure 9 — Effect of Igniter Position
(Lamp 4 cm from Surface)

paper. However, ignition did not occur at flux levels between 2.6 and 7.6 W/cm^2. This suggests that the optimum igniter wire placement cannot readily be predicted *a priori*.

Effects of Gravity and Preheating

Based on the aforementioned results, a lamp focussed at 4 cm with a Kanthal igniter 5 mm off the surface was chosen for further testing. To examine the effects of different orientations relative to the gravity vector, the orientations of Fig. 3a, 3b, and 3c were tested with the baseline parameters (4 cm, 5 mm igniter). These results are shown in Fig. 10. In addition, the preheated igniter data of Figure 7 are also shown for the *b* orientation.

Since Fig. 10 appears to show much data scatter, some explanation is needed. Figure 10 shows ignition times for Test Series **2 - 5**. For orientations *a* and *b*, one data point was suspect for each test series. One can see that the 7.0 W/cm^2 curve of Fig. 4 does not correspond with the other five profiles, suggesting a possible procedural error. This is denoted by the errant triangle in Fig. 10. Similarly, the 8.7 W/cm^2 test point of Fig. 5 was associated with an adjustment of the lamp potentiometer, and the flux varied from 0 - 8.7 W/cm^2 in the first 3 seconds. This is denoted by the

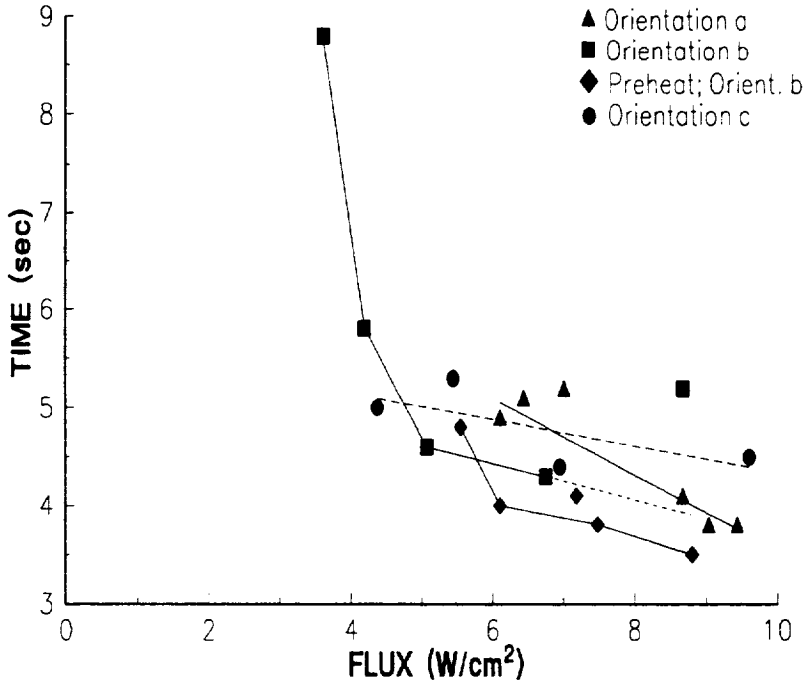

Figure 10 — Effects of Buoyancy and Preheating

errant square. Third, the 7.2 W/cm^2 curve of Fig. 7 is distinct from the other four curves, mainly in that the initial temperature was 295 K, not 320 K. This suggests that the Kanthal igniter was *not* energized 2 seconds before the lamp, as intended. Rather, Figs. 7 and 10 suggest that the igniter may have been energized only 0 - 0.5 sec before the lamp. This 7.2 W/cm^2 point is denoted by the errant diamond in Fig. 10.

It should also be noted that the three errant data points each represented the first test point in data Series 2, 3, and 5. This suggests the strong possibility of a learning curve phenomenon, since attention to detail was very important in the experimental procedure.

The orientation *c* curve of Fig. 10 shows scatter among the four data points. Considering the *c* orientation, it can be observed that buoyant flow of the volatilized fuel products is totally away from the igniter, suggesting unfavorable conditions for ignition. It is possible that the erratic profiles of Fig. 6, which differ from all other temperature profiles, are typical of the *c* orientation, but more testing is needed.

If one disregards the three errant points in Fig. 10, and accepts the unusual nature of the Fig. 3c orientation, several conclusions can be made. For the Fig. 3b orientation, preheating the igniter shortens ignition times by 0.4 - 0.5 sec. It should be noted that the symbols in Fig. 10 are sized to indicate a maximum error of ± 0.07 sec, and the 0.4 sec delta is outside of experimental error. It is also evident that ignition is most rapid, and sustainable at the lowest radiant fluxes, for the *b* orientation. Comparing the *a* and *b* curves, ignition times are similar at incident fluxes near 9 W/cm^2, but the Fig. 3b orientation is clearly advantageous below 6.5 W/cm^2. There is too much scatter in the orientation *c* data to draw definitive conclusions.

Smoldering Combustion

As discussed, ignition involves competing gas-phase and surface reactions. Hence, smoldering was briefly examined to gain further understanding of processes affecting radiative ignition.

Temperature profiles for smoldering combustion are shown in Fig. 11. The two bold curves denote the 5 cm lamp position; the other four tests are at 4 cm. As with gas-phase ignition, smoldering is indicated by a sudden increase in dT/dt. For the focussed radiation at 4 cm, the onset of smoldering occurs at 390 - 410 K. For the two 5 cm tests, the changes in dT/dt occur at 460 and 510 K. Higher temperatures at 5 cm perhaps reflect an additional 8 - 10 sec of heating. As with ignition, Fig. 12 shows that smoldering is more rapid with a focussed Gaussian lamp source.

Available O_2 at the surface can oxidize the reactive char to yield CO and CO_2, both exothermic reactions. Since both oxidation of gaseous volatiles and oxidation of char are exothermic, competing reactions consuming O_2 can exist. As Figure 11 shows, the surface reactions commence around 380 K. Since ignition does not occur until over 500 K, oxidation of char can impact ignition. It must be emphasized that potassium acetate was used to catalyze the smoldering reactions of Fig. 11. With the ignition profiles of Figs. 4 - 7, no catalyst was used, and surface reactions would be less favored. The extent to which this impacts flaming ignition is outside the scope of this review.

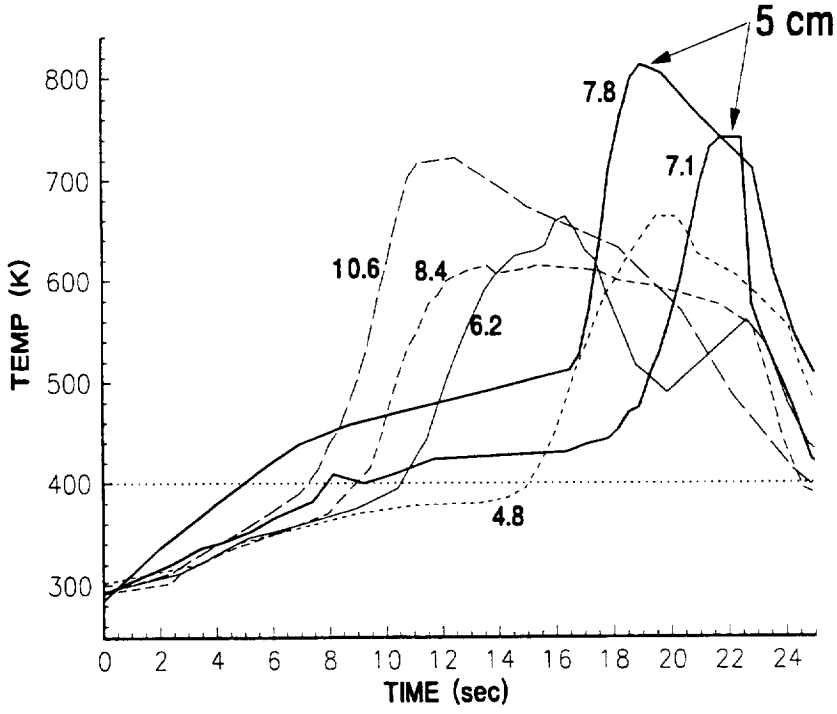

Figure 11 — Smoldering Temperature Profiles

Discussion of Results

Temperature Profiles

Closer examination of Figs. 4 - 7 yields some insight into the nature of the pyrolysis steps. All profiles show a slow, steady rise in temperature (small dT/dt) for the first 1.2 - 1.6 sec. This is due to the transient response of the halogen lamp; $\Delta T \approx 20$ K, representing sensible heating of the paper. Note that this is true for Fig. 7; although the initial temperature is higher, the delta is still 20 K. In Fig. 7, the Kanthal igniter reached 950 ± 50 K by time zero, but the temperature rise remained the same. This suggests that radiant heating by the igniter wire is experimentally insignificant, in that the lamp output overwhelms it. Although at a high temperature, the area-view factor product is very small, especially since a hole begins to burn through the paper in the first several seconds.

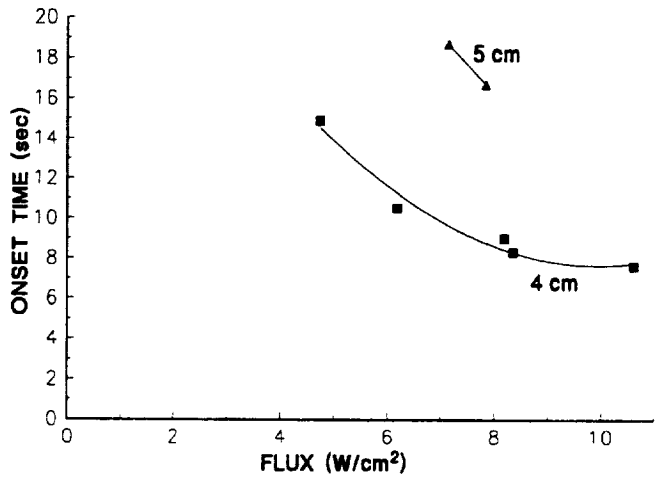

Figure 12 — Effect of Lamp Flux In Smoldering Combustion

After the initial 1.6 sec, dT/dt is approximately constant until just prior to ignition. The dT/dt value reflects several factors. With constant lamp output, a constant dT/dt reflects sensible heating of the paper. This heating decomposes the cellulose, initially yielding H_2O, CO, and CO_2. These steps are all endothermic, requiring energy and slowing the rate of sensible heating (lowering dT/dt). Just before ignition, a significantly endothermic step occurs. This can be observed as a "leveling off" of the T *vs.* t curve, representing a decrease in dT/dt (*i.e.*, $d^2T/dt^2 < 0$). This can be most easily seen in Fig. 5, but also in Figs. 4 and 7. Prior to this highly endothermic step, there is an increase in dT/dt, in the 420 - 480 K range. Since pyrolysis steps are endothermic, this increase most likely represents liberation of most of the bound water in the polymer. In similar heating of α-cellulose, Martin (*1965*) noted a change in the temperature profiles around 375 K, reflecting the beginning of water desorption.

The highly endothermic step just prior to ignition must represent release of a combustible volatile, most likely acetaldehyde, acrolein, or methanol. Shafizadeh reports that levoglucosan does not start to be vaporized until 650 - 800 K, above the temperature range of this work.

Just prior to ignition, the ordinate of Figs. 4 - 7 no longer represents a surface temperature, since a hole has burned through at the location of the thermocouple. Due to absorption of the lamp radiation by the volatiles generated, temperatures in the gas phase 1.5 mm from the surface have been measured up to 100 K higher than the surface (*Kashiwagi, 1981*). This value was measured for radiant heating of red oak, also cellulosic in nature. This ΔT is measured *before* ignition. As discussed previously, a gas-phase gradient up to 100 K/mm also exists *after* ignition.

Since it is impossible to know the surface temperature after a hole has burned through, the species volatilized just prior to ignition cannot be determined. It is assumed that acetaldehyde, acrolein, and methanol are vaporized, since subsequent ignition temperatures are consistent with the reported autoignition temperatures of these three; piloted ignition will occur before the 460, 500, and 750 K autoignition values.

It can be seen (Fig 7 *vs.* Fig. 5) that preheating alters the shape of the temperature profiles, especially after ignition. This is not understood. Preheating the igniter can radiatively heat the paper; a 20 K increase was observed. The preheating probably helps to combust volatiles which would otherwise be convected away by the 5 cm/s flow or buoyant flows. This would increase the gas temperature before ignition, which would imply a more rapid ignition, as discussed in the literature review section.

Parameters Affecting Ignition

As discussed on page 2, a flammable mixture must be present in the vicinity of the pilot igniter. These criteria are not satisfied merely by achieving a certain gas phase temperature, or by vaporizing enough ignitable volatiles in 3 or 4 seconds. Rather, the transport of the volatile species away from the igniter must be considered, as well as the availability of O_2 near the igniter. Prediction of velocity profiles near the igniter is well beyond the scope of this report. The fan moves ambient air through the flow duct at 5 cm/s, absent buoyancy. As the paper is heated, the temperature changes from 300 to 600 K in several seconds, with large density gradients and buoyant flows on the order of 30 - 100 cm/s. The plume of volatilized products rises in a direction orthogonal to the 5 cm/s air flow, for all 3 orientations tested. Given these natural and forced convective flows, O_2 must be transported to the igniter by diffusion or forced convection. A 3-dimensional O_2 gradient will exist in the flow duct, with 21% O_2 at the duct entrance. Also a factor is that the char formed during pyrolysis is highly reactive, and O_2 is chemisorbed on the surface, with char oxidation yielding CO, CO_2, and more activated sites. Thus, near the surface there can be competing demands for O_2 from the exothermic char oxidation and the exothermic oxidation of the gaseous volatiles.

As shown in Fig. 8, the focussed halogen lamp at 4 cm is preferable to the diverging beam at 5 cm, for the same total irradiance. This is, in part, because a higher temperature can be attained, and the volatile generation rate increases. With the broader 5 cm beam, temperatures are lower, ignitable volatiles are produced more slowly, and may be transported from the igniter before a flammable mixture can accumulate. Thus, a higher total irradiance will be needed at 5 cm to achieve ignition within a specified time, as the curves show. Similarly, since there is an ignition threshold, denoted by "NO IGNITION" in Figs. 8 and 9, the minimum power necessary for ignition will also be higher. The 5 cm data suggests that ignition must occur within 10 seconds—beyond that, volatiles produced will dissipate without attaining a flammable mixture.

Other investigators have observed behavior similar to that of Fig. 8. In radiant heating of red oak at 8 - 18 W/cm^2, Kashiwagi (*1979*) found that the type of radiant source affected the results. In that case, ignition occurred more readily with a halogen lamp than with a laser. This suggests there is a limit to focussing a source; a highly focussed laser may burn a hole through the fuel too quickly, without heating a large enough area to generate a sufficient plume of ignitable products. Ignition times for red oak also increased more rapidly at lower irradiances. Similarly, Simms (*1963*) observed that ignition times for piloted ignition of wood increased rapidly below 3 W/cm^2; at higher fluxes, the curve was nearly linear. This observation is very similar to the results in Figs. 8 and 10. Recent computer modelling (*McGrattan, 1995*) using parameters very similar to the present work found that ignition is achieved most rapidly with a sharp (*i.e.,* focussed) flux distribution, as Fig. 8 indicates.

Given that a focussed heat source is preferable, the optimum gas-phase location of the igniter was next investigated. A Kanthal igniter in contact with the fuel is optimum; however, this heats

the fuel by radiation, convection, and conduction, and compromises the study of radiative ignition. Figure 9 shows that a location 5 mm away is more optimal than 3 - 3.5 mm. This finding is quite surprising and unexpected. The 5 mm results are reproducible; as Fig. 10 shows, observed ignition times correlate well with changes in experimental parameters.

One explanation is that an ignitable mixture is easier to attain slightly farther from the surface. Martin (*1965*) found that the initial volatile composition in thermally irradiated α-cellulose was 96 wt% CO, CO_2, and H_2O, with acetaldehyde and methanol being the main ignitable volatiles. Since CO, CO_2, and H_2O are liberated first, they may be transported away from the surface somewhat by the buoyant plume. The presumed ignitables are nonetheless present initially in small quantities. Furthermore, there is a gradient of O_2 within the flow duct. Although the velocity profiles are unknown, it is reasonable that the O_2 level would be higher farther from the surface, for at least two reasons. One, close to the surface there is competition for the available O_2 from the char oxidation reactions. Second, the buoyant flows transport ignitable species away from the surface. Since these buoyant flows are an order of magnitude higher than the 5 cm/s flow of air, O_2 must diffuse to the igniter region in the presence of dominant buoyant flow of fuels. It is thus possible that higher levels of O_2 exist 5 mm from the surface than are present at 3 mm. Although somewhat intractable, computer modelling could possibly verify this hypothesis.

This hypothesis cannot explain why ignition could be achieved at lower irradiance levels at the 3 mm location. Closer to the surface, a lower O_2 level would suggest a lower N_2 level as well, assuming no O_2 is produced at the paper surface. This question is unresolved, and could be the focus of additional research.

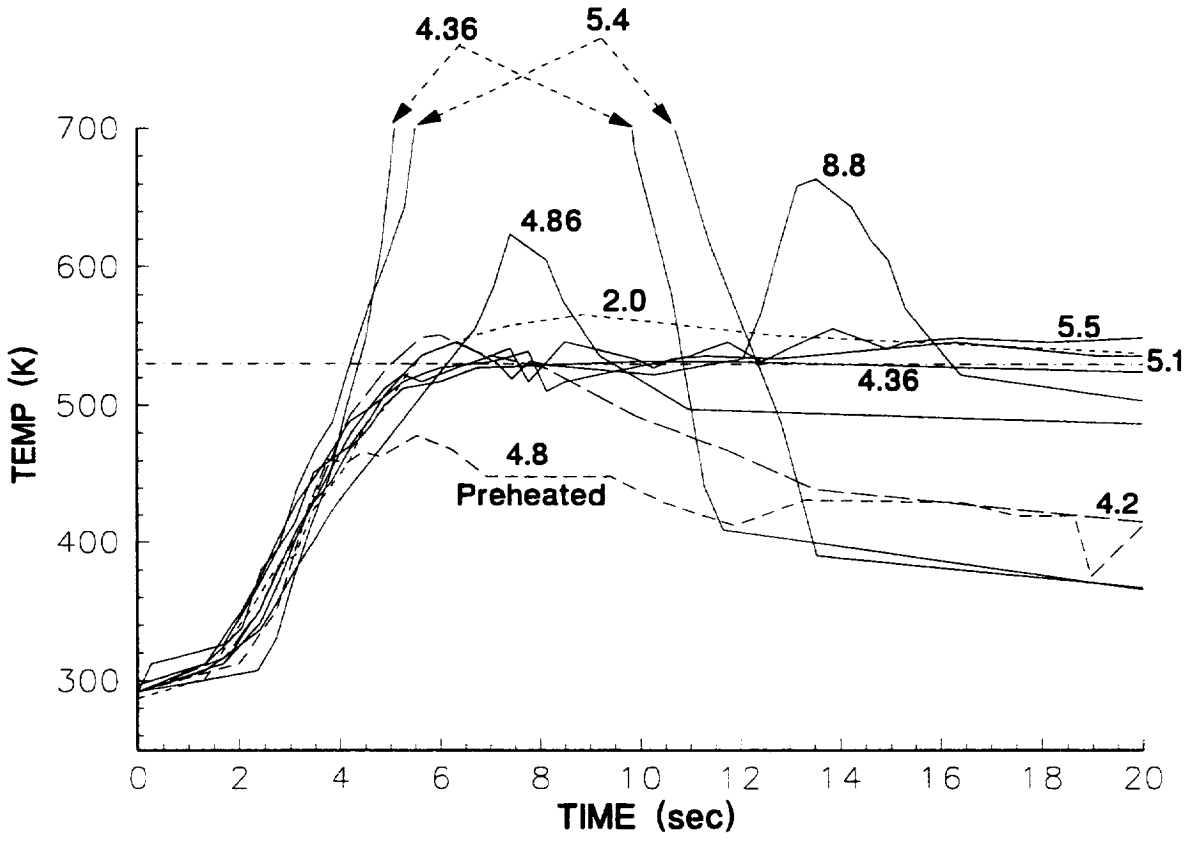

Figure 13 — Non-Ignition Temperature Profiles

Effects of Gravity Vector

Further insight into buoyant effects is gained from an inspection of temperature profiles where ignition did *not* occur. Temperature profiles for eight non-ignition cases are shown in Fig. 13, with two successful (*i.e.*, ignition) tests shown for comparison. Ignition was difficult to reproduce for the Series **4** tests, which are denoted in Fig. 13 by solid lines. As shown, ignition was achieved at 4.4 and 5.4 W/cm^2, and the peaks after ignition were above 1300 K. However, in other tests in the *c* orientation, ignition did not occur at 4.4, 4.9, 5.1, 5.5 and 8.8 W/cm^2.

Ignition was observed to occur between 510 and 650 K. For the two ignition cases of Fig. 13, ignition was achieved near 640 K. (Ignition temperatures are discussed below). As indicated by the reference line, a quasi-steady state reading near 530 K was typical for non-ignition cases. Notably, for the 4.9 and 8.8 W/cm^2 curves, peak temperatures of 620 and 660 K were attained, but without ignition. Since ignition was achieved below 650 K more than 50 times, it is evident that a specified temperature cannot be used as a guarantee of ignition.

As discussed on page 2, three criteria are necessary for ignition. Since the traces of Fig. 13 are very similar for 4 sec, one must assume that cellulosic decomposition is similar as well, and that sufficient volatiles are generated in all cases. Further, the 4.9 and 8.8 W/cm^2 curves show that a temperature typical of ignition was achieved. These curves suggest that a flammable mixture began to oxidize, with an exothermic burst lasting 2 or 4 seconds. That is, for these two cases, a flammable mixture at a suitably high temperature was available, satisfying criteria (1) and (2) for ignition.

The most compelling explanation for the 4.9 and 8.8 W/cm^2 cases is that heat losses from the gas phase were sufficiently high that ignition could not be sustained, with criterion (3) not satisfied. This could occur for several reasons. One, the rate of generation of volatiles could be too low to sustain ignition. This seems feasible for the 8.8 W/cm^2 test; when the mixture ignited after 12.5 sec, the most volatile species would have dissipated. Two, ignition could not be achieved or sustained if the flow of volatile species was away from the igniter, even if sufficient volatile species were generated. Inspection of Fig. 3c shows that buoyant flow would transport all volatile species away from the igniter. Even on the downward side of the paper, facing the igniter, any volatiles formed would "jet" through the hole already burned in the paper.

Given that buoyant flows for the *c* configuration were away from the igniter wire, it should not be surprising that ignition was difficult to achieve and reproduce. Thus, although ignition occurred at 4.4, 5.4, 7.0 and 9.6 W/cm^2, in other tests it was **not** achieved in the 4.4 - 8.8 W/cm^2 range. This finding and Fig. 10 indicate convincingly that buoyant flows are quite important in the ignition process. Furthermore, although a sufficient flow of volatiles may be achieved, and the temperature may be high, ignition cannot occur if volatiles are not transported to the pilot igniter. At much higher flux levels, the mixture could autoignite, and buoyant flows would become less important to ignition.

Given the above, the trends shown in Fig. 10 are better understood. (Symbol size denotes a ±0.07 sec uncertainty in ignition time). Because of the factors discussed, significant scatter in the *c* data is not surprising. Conversely, the *b* orientation allows for transport of volatilized products directly to the Kanthal igniter. Thus, more rapid ignition, and sustained ignition at lower irradiances, would be expected, as denoted by the squares and diamonds. The *a* orientation, by contrast, placed the fuel sample in a vertical orientation. Inspection of Fig. 3 suggests intuitively that the *a* configuration is less favorable than *b*. As Fig. 10 indicates, ignition is slower at 6

W/cm^2, but approaches the *b* curves near 9 W/cm^2. This would seem to indicate that buoyant flows become somewhat less important as the irradiance level rises. As irradiance increases, volatile generation increases, and the gas phase temperature will be higher, enabling ignition. Comparison of the vertical fuel sample data (*a*) with the *c* data is more difficult, given the large data scatter shown by the oval symbols. The Fig. 3b orientation is clearly favored over the 3a and 3c orientations, as one would expect.

Effects of buoyant transport on ignition have been reported previously. Kashiwagi (*1981*) noted that a "horizontal sample orientation causes the strongest interaction between external radiation and the decomposition products." He further noted that a vertical orientation (*e.g.*, Fig. 3a) would demonstrate different behavior. The boundary layer of decomposition products in a vertical sample will be thinner than the buoyant plume from a horizontally mounted sample (Fig. 3b). If the buoyant plume absorbs any incident radiation, the gas-phase volatiles will be heated more with a horizontal sample (plume) than those rising from a vertical sample, which has a thin boundary layer of volatiles. Kashiwagi (*1979*) presented experimental data quantifying these effects. One would thus expect ignition to be achieved more readily in a horizontal sample, as was indicated in the *b* orientations of Fig. 10.

As mentioned, preheating the igniter shortens ignition times by 0.4 - 0.5 sec when tested in the favorable *b* orientation. Comparison of Figs. 5 and 7 shows that preheating markedly changes the temperature profiles, especially after ignition. Similarly, the dashed curve labeled "Preheated" in Fig. 13 shows that thermal behavior in a non-ignition case deviates substantially, and a lower maximum temperature is achieved. Further insight is gained from Fig. 14, discussed below. Comparison of the two curves labeled "4, 5 mm,b" indicates a considerable change in ignition temperature behavior when the igniter is preheated for 2 sec before energizing the halogen lamp.

Figures 6, 7, 13, and 14 indicate that preheating must somehow alter the pyrolysis of cellulose. The only physical difference in preheating is that the igniter effectively reaches its steady-state temperature 2 sec sooner, and the igniter is already above 900 K when the lamp is energized. Since the lamp does not reach steady state for ≈ 1.2 sec, the heating profile is altered slightly for at least 3.2 sec. This has two effects. One, there is a small radiant heating contribution from the Kanthal wire. Two, and more significantly, any volatilized species generated in the first 3.2 sec will experience a higher temperature in the vicinity of the igniter. Although Martin's (*1965*) results indicate that CO, CO_2, and H_2O may constitute more than 95% (by weight) of the initial gaseous species, there would nonetheless be traces of acetaldehyde, acrolein, methanol, and perhaps furan, assuming the applicability of his results. Thus, even if the gaseous mixture did not ignite, any oxidation of these combustibles would be exothermic, increasing the gas and surface temperatures, and enabling ignition at shorter times. (Although the radiant interchange from a 30 gauge wire to a 25 mm disk 5 mm away could be calculated, Fig. 7 suggests that this value is on the order of 20 - 30 K).

Temperature at Ignition

Since temperature has been used as a criterion for ignition, the temperatures observed herein are shown in Fig. 14. Here, a label such as "4, 3 mm, a" refers to the 4 cm lamp position, with the pilot 3 mm away, tested in the Fig. 3a orientation. The temperatures plotted are those at the "Point of Ignition" shown in Fig. 4. Recall that a hole always burned through the paper at the focal point of the lamp. At this point, because of the Gaussian distribution, the maximum flux was approximately a factor of three greater than the average flux (averaged over the 2.80 cm^2 spot size

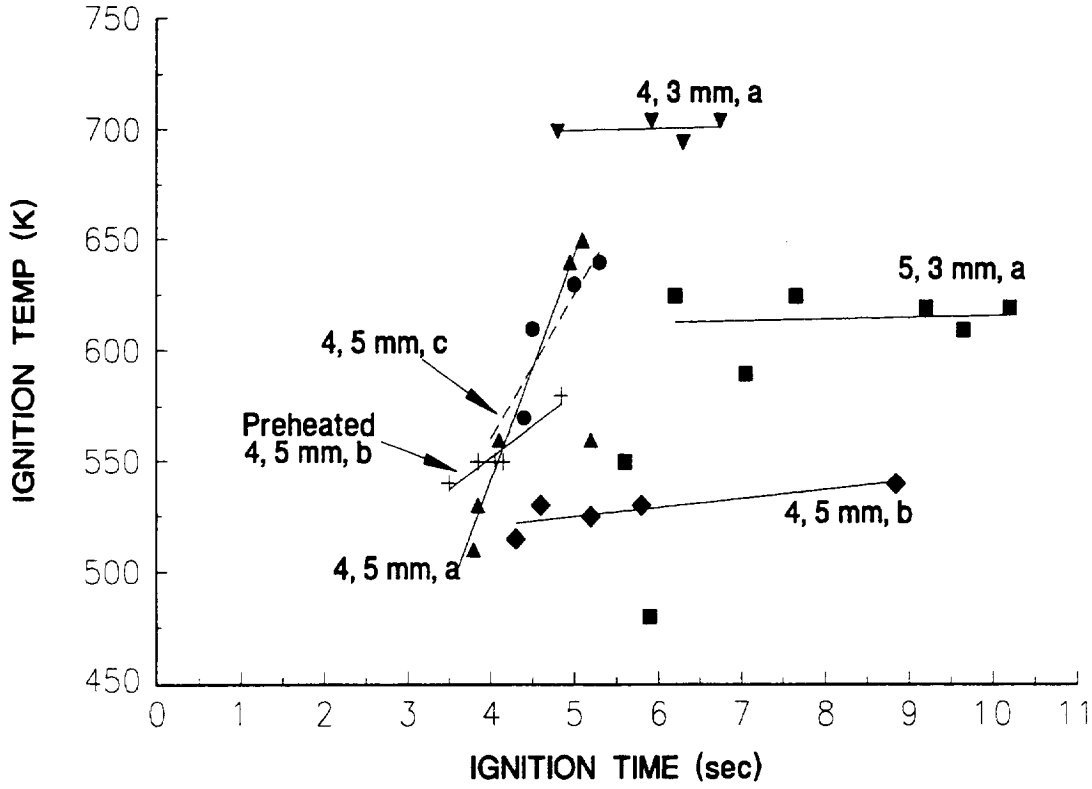

Figure 14 — Observed Ignition Temperatures

at the 4 cm location). The hole rapidly grew, releasing gaseous species until ignition occurred. Due to the high flux at the focal point, the thermocouple bead was positioned offset about 1 cm from the lamp focal point, to minimize radiant heating of the thermocouple. Thus, at ignition, the thermocouple indicated a gas-phase temperature on the centerline of the paper, but in an area of lower lamp irradiance.

Caution must be exercised in drawing conclusions from Fig. 14, since gas-phase temperatures are indicated. As mentioned, gradients of 100 K/mm have been observed in the gas-phase at ignition. Before ignition, gas-phase temperatures can be 100 K higher than at the surface (*Kashiwagi, 1981*), due to absorption of radiation. Nonetheless, the contributions of these factors will be very similar for a specific series of tests (*cf.* Table I), although there may be differences between test series, due to differing buoyant flows.

Figure 14 shows that ignition temperature is nearly constant at the 3 mm igniter position. Ignition occurs around 700 K at the 4 cm distance, but around 620 K at 5 cm. This may largely reflect the fact that the paper surface reaches higher temperatures at the 4 cm focal length of the lamp, although the rate of gaseous species released also changes.

For unknown reasons, ignition temperature varies at the 5 mm pilot location. One immediately notices that the *b* orientation shows different temperature dependence, further evidence that buoyant transport of gaseous species away from the paper is very important. Preheating the igniter in the *b* orientation clearly changes behavior, further circumstantial evidence that preheating the pilot igniter substantially affects the ignition process.

Given that positioning error for the pilot igniter was up to ±0.5 mm, and thermocouple position could vary as much as ±0.5 mm (0.3 mm likely), an uncertainty of 30 K in ignition temperature is

very possible. One could thus conclude that three of the "4 cm, 5 mm" lines are better fitted by one least-squares line, although there is no fundamental reason for doing this.

Many of the results indicated in Fig. 14 are poorly understood. In future work, a sample holder unaffected by 1300 K temperature differences could be employed. Similarly, thermocouples sufficiently tensioned and positioned to maintain position within ±0.1 mm between 300 and 1600 K could be employed to better investigate the temperature at ignition. This was beyond the scope of this investigation.

Even given the experimental uncertainty, Fig. 14 clearly indicates that temperature cannot be used as a general ignition criterion. As Fig. 13 indicates, temperatures of 620 and 660 K were attained in two non-ignition cases.

Comparison with Previous Work

Ignition of cellulosic materials has been investigated by numerous researchers. The incident irradiance herein varied from 2 - 10 W/cm^2. This area-averaged flux considers an elliptical spot containing 86% of the incident power; lower fluxes outside the ellipse are considered insignificant. Conversely, the peak flux of the Gaussian distribution is approximately twice this average flux.

Numerous researchers have reported a constant ignition criteria for cellulose. In a review of ignition of cellulosic materials (*Weatherford, 1965*), a 620 K ignition temperature is derived. At large irradiances between 21 and 67 W/cm^2, Martin (*1965*) reported surface temperatures between 870 and 920 K for non-piloted ignition of α-cellulose. The same 920 K value for autoignition was observed by Bamford, as referenced elsewhere (*Weatherford*). Weatherford also reports autoignition thresholds as high as 1270 K. At these high fluxes, autoignition of cellulose is controlled by gas phase heat transfer (*Martin*), and theoretical considerations predict a constant ignition temperature. By contrast, at the very low heat fluxes of this work, ignition is largely controlled by heat transfer to the paper, such that sufficient generation of volatiles occurs.

Variation of ignition temperature for cellulosic materials has been reported elsewhere. Figure 14 indicates that ignition temperature increases with ignition time, meaning that it *decreases* with increasing irradiance, per Figs. 8 - 10. Kashiwagi (*1979*) reported this same trend for piloted and autoignition of red oak, at fluxes of 7 - 17 W/cm^2. Although his data was best fit with a 2nd order polynomial, the dependence is nearly linear over intervals comparable to Figs. 8 - 10. Kashiwagi attributed this dependence to the varying degree of importance of gas-phase absorption of radiation, as opposed to the higher surface temperatures after longer heating periods. He also reported that ignition temperature dependence is different for vertical and horizontal samples (*cf.* Figs. 3a, 3b). This is attributed to changing boundary layer behavior as orientation is changed.

It is thus seen that piloted ignition of cellulose can occur as much as 300 K lower than autoignition. The dependence of pilot location on ignition time, observed herein, has also been noted by Simms (*1963*). In his work, similar flux levels were used in the radiant heating of wood samples. The distance of a gas pilot flame from the surface ranged from 6.2 to 19 mm. There, the pilot flame was 12.5 mm long, and burned downwards from the gas supply. Simms observed that ignition time increased as the pilot flame was positioned farther from the surface.

The present finding that ignition occurred more rapidly at a 5 mm pilot location than at 3 mm must be further investigated. The hypothesis advanced of a deficiency of O_2 close to the surface is untested. Furthermore, although the author has a high degree of confidence in the repeatability of the 5 mm results, less testing was done at the 3 mmlocation. More testing at variable pilot locations would be needed for better insight into the effects of pilot location.

Conclusions

The experimental results discussed above clearly show that ignition times decrease as the irradiance level increases. This ignition time is governed by the precise manner of heating the fuel sample. A more concentrated source is clearly preferred to increase surface temperature and volatile generation rate. The presence of a pilot igniter enables ignition at much lower temperatures, as well as lower external flux levels. The location of a pilot igniter relative to the surface substantially affects the ignition process, but the reasons for this are not understood. Determination of the optimal pilot location was not resolved herein.

For the low irradiances investigated (2 - 8.5 W/cm^2), ignition temperature varies considerably, depending on flux level, orientation of the gravity vector, and pilot location. The results clearly indicate that a specified temperature cannot be used as a criterion for low-flux ignition of cellulose. Instead, ignition is determined by the existence of a flammable mixture at the pilot igniter. Sustained ignition is dependent on sufficiently low heat losses from the flame. If buoyant flows transport combustible volatiles away from a pilot source, ignition cannot be sustained even if sufficient volatiles are otherwise generated. Hence, radiative ignition is enhanced when the sample is oriented such that buoyant flows of volatile products rise toward a high temperature pilot source.

Acknowledgements

The author is indebted to Sandra Olson for her role in advocating this experimental effort, and for her numerous suggestions throughout. Dan Sokol (presently at Cornell University) conducted the flux gage calibrations of the tungsten-halogen lamp, and provided valuable assistance with selected experimental tasks.

REFERENCES

Eckbreth, A.; Laser Diagnostics for Combustion Temperature and Species, Abacus Press, 1988.

Glassman, I.; Combustion, 2nd edn., Academic Press, 1987.

Kashiwagi, T.; *Combust. Flame*, 34, 231 - 244, 1979.

Kashiwagi, T.; *Fire Safety J.*, 3, 185 - 200, 1981.

Kashiwagi, T. *et. al.*; *Combust. Flame*, 69, 331 - 345, 1987.

Kashiwagi, T. and Nambu, H.; *Combust. Flame*, 88, 345 - 368, 1992.

Martin, S.; *Tenth Symposium (International) on Combustion*, 877 - 896, The Combustion Institute, 1965.

McGrattan, K.B., *et. al.*, *Effects of Ignition and Wind on the Transition to Flame Spread in a Microgravity Environment, Combust. Flame,* (to appear Sept. 1996).

Olson, S.L.; *Combust. Sci. Technol.*, 76, 233 - 249, 1991.

Sacksteder, K.R. and T'ien, J.S.; *Twenty-Fifth Symposium (International) on Combustion*, 1685 - 1692, 1994.

Shafizadeh, F; *The Chemistry of Pyrolysis and Combustion*, in The Chemistry of Solid Wood, Amer. Chem. Soc., Washington, 1984.

Siegel, R. and Howell, J.R.; Thermal Radiation Heat Transfer, 2nd edn., McGraw-Hill, 1981.

Simms, D.L.; *Combust. Flame*, 7, 253 - 261, 1963.

Weatherford, W.D. and Sheppard, D.M.; *Tenth Symposium (International) on Combustion*, pp. 897 - 910, The Combustion Institute, 1965.

REPORT DOCUMENTATION PAGE

Form Approved
OMB No. 0704-0188

1. AGENCY USE ONLY (*Leave blank*)	2. REPORT DATE	3. REPORT TYPE AND DATES COVERED
	August 1996	Technical Memorandum

4. TITLE AND SUBTITLE

Ignition of Cellulosic Paper at Low Radiant Fluxes

5. FUNDING NUMBERS

WU-963-80-0A

6. AUTHOR(S)

K. Alan White

7. PERFORMING ORGANIZATION NAME(S) AND ADDRESS(ES)

National Aeronautics and Space Administration
Lewis Research Center
Cleveland, Ohio 44135-3191

8. PERFORMING ORGANIZATION REPORT NUMBER

E-10405

9. SPONSORING/MONITORING AGENCY NAME(S) AND ADDRESS(ES)

National Aeronautics and Space Administration
Washington, D.C. 20546-0001

10. SPONSORING/MONITORING AGENCY REPORT NUMBER

NASA TM-107311

11. SUPPLEMENTARY NOTES

Responsible person, K. Alan White, organization code 6742, (216) 433-6563.

12a. DISTRIBUTION/AVAILABILITY STATEMENT

Unclassified - Unlimited
Subject Categories 25 and 34

This publication is available from the NASA Center for AeroSpace Information, (301) 621-0390.

12b. DISTRIBUTION CODE

13. ABSTRACT (*Maximum 200 words*)

The ignition of cellulosic paper by low level thermal radiation is investigated. Past work on radiative ignition of paper is briefly reviewed. No experimental study has been reported for radiative ignition of paper at irradiances below 10 Watts/ cm^2. An experimental study of radiative ignition of paper at these low irradiances is reported. Experimental parameters investigated and discussed include radiant power levels incident on the sample, the method of applying the radiation (focussed *vs.* diffuse Gaussian source), the presence and relative position of a separate pilot ignition source, and the effects of natural convection (buoyancy) on the ignition process in a normal gravity environment. It is observed that the incident radiative flux (in W/cm^2) has the greatest influence on ignition time. For a given flux level, a focussed Gaussian source is found to be advantageous to a more diffuse, lower amplitude, thermal source. The precise positioning of a pilot igniter relative to gravity and to the fuel sample affects the ignition process, but the precise effects are not fully understood. Ignition was more readily achieved and sustained with a horizontal fuel sample, indicating the buoyancy plays a role in the ignition process of cellulosic paper. Smoldering combustion of doped paper samples was briefly investigated, and results are discussed.

14. SUBJECT TERMS	15. NUMBER OF PAGES
Ignition; Cellulose; Radiative ignition	28
	16. PRICE CODE: A03

17. SECURITY CLASSIFICATION OF REPORT	18. SECURITY CLASSIFICATION OF THIS PAGE	19. SECURITY CLASSIFICATION OF ABSTRACT	20. LIMITATION OF ABSTRACT
Unclassified	Unclassified	Unclassified	

National Aeronautics and
Space Administration

Lewis Research Center
21000 Brookpark Rd.
Cleveland, OH 44135-3191